Purcell-modified Doppler cooling of quantum emitters inside optical cavities

J. Lyne [1,2] N. S. Bassler [1,2] S. Park [3] G. Pupillo [4] and C. Genes [2,1]
[1]*Department of Physics, Friedrich-Alexander-Universität Erlangen-Nürnberg, Staudtstraße 7, D-91058 Erlangen, Germany*
[2]*Max Planck Institute for the Science of Light, Staudtstraße 2, D-91058 Erlangen, Germany*
[3]*Daegu Gyeongbuk Institute of Science and Technology, 333 Techno jungang-daero, Hyeonpung-eup, Dalseong-gun, Daegu, South Korea*
[4]*Centre Européen de Sciences Quantiques (CESQ), Institut de Science et d'Ingénierie Supramoléculaires (ISIS) (UMR7006) and Atomic Quantum Computing as a Service (aQCess), University of Strasbourg and CNRS, Strasbourg 67000, France*

(Received 22 January 2024; accepted 31 May 2024; published 17 July 2024)

Standard cavity cooling of atoms or dielectric particles is based on the action of dispersive optical forces in high-finesse cavities. We investigate here a complementary regime characterized by large cavity losses, resembling the standard Doppler cooling technique. For a single two-level emitter a modification of the cooling rate is obtained from the Purcell enhancement of spontaneous emission in the large cooperativity limit. This mechanism is aimed at cooling quantum emitters without closed transitions, which is the case for molecular systems, where the Purcell effect can mitigate the loss of population from the cooling cycle. We extend our analytical formulation to the many-particle case governed by small individual coupling, but exhibiting large collective coupling.

DOI: 10.1103/PhysRevA.110.013115

I. INTRODUCTION

There are many ways to control the motion of atomic-sized objects via laser light and progress in cooling ions, and atoms have seen the emergence of techniques such as Doppler laser cooling, resolved sideband cooling, evaporative cooling, sub-Doppler cooling, and so on [1–4]. In general, these techniques make use of a cooling cycle between two electronic states where quick cycling of laser photons followed by many spontaneous emission events (at rate γ) removes kinetic energy into the electromagnetic bath. There are also alternatives which employ the enhanced coupling between a single photon and a single atom allowed by the use of optical cavities, i.e., within the cavity quantum electrodynamics (cQED) formalism [5–8]. Operation in a dispersive regime circumvents spontaneous emission and kinetic energy is removed via the loss of cavity photons (at rate κ) as proposed and discussed [9–12] and experimentally realized both for single atoms [13,14] as well as for ensembles [15,16].

Most of these techniques are not optimal for the cooling of molecules owing to their large number of vibrational and rotational sublevels where the population can migrate from the cooling cycle and thus reduce the cooling performance. In the context of cavity cooling, difficulties and mitigation solutions have been extensively discussed [17]. In other contexts, progress has been made in laser cooling of the center of mass of small molecules such as diatomics (CaF and SrF) [18–21], symmetric tops ($CaOCH_3$) [22], and asymmetric top molecules [23].

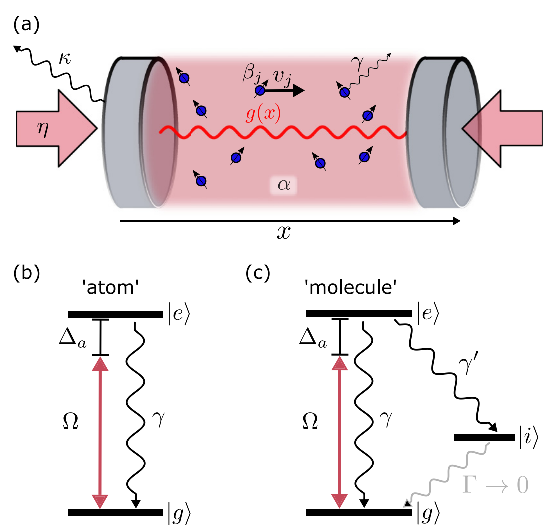

FIG. 1. (a) A variation of a standard one-dimensional Doppler cooling scheme for many emitters. Each emitter moves with some velocity v_j and the coupling between emitter coherence β_j and the cavity mode α is spatially dependent via $g(x_j)$, where g is the light-matter coupling constant. The cavity is driven with amplitude η. Spontaneous emission at rate γ and photon loss at rate κ are assumed. We consider two types of electronic level schemes for the emitters. (b) Electronic level scheme of a closed two-level system with energy eigenstates $|e\rangle$ (excited) and $|g\rangle$ (ground). Driving with amplitude Ω and detuning Δ_a is assumed. (c) Possible electronic level scheme mimicking a molecule with an additional level $|i\rangle$ to which population is lost from the cycle transition (with negligible repopulation rate Γ).

Published by the American Physical Society under the terms of the Creative Commons Attribution 4.0 International license. Further distribution of this work must maintain attribution to the author(s) and the published article's title, journal citation, and DOI. Open access publication funded by Max Planck Society.

We investigate here a hybrid scenario of Doppler-like cooling inside an optical cavity in the dissipative regime, where the rate of spontaneous emission of an atom or molecule is enhanced when operating in the Purcell regime of cQED, i.e., in the bad-cavity regime. This is inspired by experiments showing that the branching ratio of spontaneous emission in molecules can be strongly manipulated via optical cavities [24], albeit in solid-state environments where molecules are fixed in a host matrix. Extending this argument to molecules in a gas phase or in solvents can provide a mechanism to increase the cycling of photons and thus *close* the cooling cycle by reducing the rate of population loss into additional rotational or vibrational levels. We do not utilize dispersive optical forces as in standard cavity cooling, but simply employ the cavity as an additional dissipation channel for the emitters. This intuition is indeed validated for single quantum emitters, both with closed and nonclosed transitions in the regime where the cavity cooperativity is larger than unity. However, we find that extensions to many-particle systems, where the Purcell effect stems from a collective coupling to the cavity mode, indicates that individual loss of energy is not positively affected by collective properties. Our aim is solely in deriving a modified cooling or slowing down rate and to identify the mechanism via which the cavity can enhance it. The question of final temperature is not included in our formalism.

The paper is organized as follows. In Sec. II we proceed with computing analytical expressions for the cooling rates of quantum emitters with either closed or nonclosed transitions inside the one-dimensional geometry illustrated in Fig. 1. The results are compared to the standard situation of Doppler cooling in free space in the counterpropagating wave geometry. We identify the emitter-cavity cooperativity $\mathcal{C} = g^2/(\kappa\gamma)$ as the main tuning knob for speeding up the cooling process and maximizing the cooling time (for nonclosed transitions) with $\mathcal{C} \gg 1$. We then generalize in Sec. III to the many-particle case, where the single-particle cooperativity is small ($\mathcal{C} \ll 1$), but the collective cooperativity is large ($\mathcal{N}\mathcal{C} \gg 1$). We derive analytical results for the cooling rate of each particle, which indicate that the collective Purcell regime with $\mathcal{N}\mathcal{C} \gg 1$ does not positively affect the loss of kinetic energy at the individual particle level.

II. SINGLE-PARTICLE COOLING

Consider a one-dimensional scenario of a moving two-level system of mass m with an electronic transition between the ground state $|e\rangle$ and excited state $|g\rangle$ with frequency separation ω_0. We will first address the standard Doppler cooling scenario for a closed transition system in a standing wave. We refer to a closed transition system as one consisting of only two levels as in Fig. 1(b) where the excited state can undergo spontaneous emission only to the ground state. Next we consider the effect of placing the closed system within the confined electromagnetic volume of an optical cavity. We then depart from the closed system description by including an additional level in the electronic structure, which is exclusively populated via spontaneous emission from the excited state [see Fig. 1(c)]. We refer to the system as a nonclosed transition system. Again, we consider free space and cavity scenarios.

In the standard understanding of Doppler cooling, the condition of red-detuning $\Delta_a = \omega_0 - \omega_\ell > 0$ of the laser beam at frequency ω_ℓ with respect to the electronic transition is required. The cooling mechanism consists of the stimulated absorption of a photon below the resonance frequency, followed by spontaneous emission at the natural frequency. The energy difference then translates into a loss of kinetic energy and thus cooling. To derive a cooling rate, a semi-classical approach suffices, where an effective drag coefficient for the particle's momentum is derived that shows dependence on the driving power, detunings, and spontaneous emission rate. We start by reviewing such fundamental steps which we then expand to include the cavity scenario for both closed and nonclosed transition systems as depicted in Figs. 1(b) and 1(c).

The derivation is based on stating the master equation for the quantum emitter including motion from which we derive the equations of motion of the classical expectation values. Electronic transitions are described by the Pauli ladder operator $\hat{\sigma} = |g\rangle\langle e|$ and its Hermitian conjugate. The free Hamiltonian is

$$\hat{\mathcal{H}}_0 = \frac{\hat{p}^2}{2m} + \hbar\Delta_a\hat{\sigma}^\dagger\hat{\sigma}, \tag{1}$$

consisting of the kinetic energy operator and the two-level system Hamiltonian in a frame rotating with the laser frequency ω_ℓ, which we specify later. The spontaneous emission at rate γ is incorporated as a Lindblad superoperator

$$\mathcal{L}_{\mathrm{em}}[\hat{\rho}] = \gamma[2\hat{\sigma}\hat{\rho}\hat{\sigma}^\dagger - \hat{\sigma}^\dagger\hat{\sigma}\hat{\rho} - \hat{\rho}\sigma^\dagger\hat{\sigma}]. \tag{2}$$

The rate of spontaneous emission given by $\gamma = \omega_0^3 d_{eg}^2/(6\pi c^3\varepsilon_0)$ where d_{eg} is the transition dipole matrix element, ε_0 denotes the vacuum permittivity, and c is the speed of light in the vacuum. The dynamics of the system are then described by a master equation $\mathrm{i}\dot{\hat{\rho}} = [\hat{\mathcal{H}}_0, \hat{\rho}]/\hbar + \mathcal{L}_{\mathrm{em}}[\hat{\rho}]$ for the system's density operator $\hat{\rho}$. The approach in terms of a Lindblad master equation as written in Eq. (2), neglects the effect of recoil in spontaneous emission. We will only consider operator averages and due to the isotropy of spontaneous emission, no momentum is imparted onto the emitter on average. However, the momentum imparted onto the emitter in spontaneous emission has nonzero variance, which results in a limit on the final temperature (Doppler temperature). We do not derive any modified temperature limits.

A. Free-space Doppler cooling of a closed transition system

Adding a classical laser drive with frequency ω_ℓ and Rabi frequency Ω with a standing wave spatial structure leads to a position-dependent Rabi frequency $\Omega(x) = \Omega\cos(k_\ell x)$. In a frame rotating at ω_ℓ, the time-independent Hamiltonian becomes

$$\hat{\mathcal{H}} = \hat{\mathcal{H}}_0 + \hbar\Omega(\hat{x})[\hat{\sigma} + \hat{\sigma}^\dagger]. \tag{3}$$

The dynamics of the expectation values of system operators such as $\beta = \langle\hat{\sigma}\rangle$, $p = \langle\hat{p}\rangle$, and $x = \langle\hat{x}\rangle$ can be deduced from the master equation with $\hat{\mathcal{H}}$ as the total system Hamiltonian

$$\dot{\beta} = -(\gamma + \mathrm{i}\Delta_a)\beta - \mathrm{i}\Omega(x), \tag{4a}$$

$$\dot{p} = -\hbar\Omega'(x)[\beta + \beta^*], \tag{4b}$$

$$\dot{x} = p/m. \tag{4c}$$

We made the low-excitation approximation where $\langle\hat{\sigma}^\dagger\hat{\sigma} - \hat{\sigma}\hat{\sigma}^\dagger\rangle \approx -1$ and factorized quantum correlations between motional and internal degrees of freedom $\langle\hat{x}\hat{\sigma}\rangle = \langle\hat{x}\rangle\langle\hat{\sigma}\rangle$. To solve the equation of motion for the emitter coherence β we perform a Floquet expansion in the spatial harmonics of the driving field $\beta = \sum_{n=-\infty}^{\infty} b_n e^{\mathrm{i}nk_\ell x}$, where the coefficients b_n are still time dependent. However, we assume that the expansion coefficients are stationary, which is a good approximation as long as the cooling rate is small compared to the rate of spontaneous emission γ. Inserting the expansion into the equation of motion Eq. (4a) gives only nonzero contributions for the harmonics of first order, i.e., b_n with $n = \pm 1$, which are not coupled in free space. We obtain the following set of equations:

$$b_n[\gamma + \mathrm{i}(\Delta_a + nk_\ell v)] = -\frac{\mathrm{i}\Omega}{2}(\delta_{n,+1} + \delta_{n,-1}), \tag{5}$$

where $v = \dot{x}$ is the instantaneous velocity of the emitter. The equations are solved by the following coefficients:

$$b_{\pm 1} = \frac{-\mathrm{i}\Omega}{2[\gamma + \mathrm{i}(\Delta_a \pm k_\ell v)]}. \tag{6}$$

For small Doppler shifts $k_\ell v \ll \Delta_a$, the coefficients may be approximated by

$$b_{\pm 1} \approx \frac{-\mathrm{i}\Omega}{2[\gamma + \mathrm{i}\Delta_a]} \pm \frac{-\Omega}{2[\gamma + \mathrm{i}\Delta_a]^2} k_\ell v \tag{7}$$

up to first order in $k_\ell v/\Delta_a$. The equation for the motion of the emitter momentum contains products of the gradient of the oscillating drive $\Omega'(x)$ and the oscillating emitter coherence $\beta(x)$. This leads to the occurrence of both constant terms and terms which oscillate at two times the fundamental spatial frequency of the standing wave. The constant term is a spatially independent force proportional to the emitter velocity (cooling force) and on timescales larger than half of the Doppler period $\pi/(k_\ell v)$ the oscillating terms average out, such that merely the cooling force remains. This results in an exponential decay of the emitter velocity $\dot{v} \approx -\xi_{\mathrm{fs}} v$. With the introduction of the recoil frequency $\omega_{\mathrm{rec}} = \hbar k_\ell^2/(2m)$, the cooling rate takes the following standard expression [25–29]:

$$\xi_{\mathrm{fs}} = \frac{4\Omega^2\omega_{\mathrm{rec}}\Delta_a\gamma}{\left[\gamma^2 + \Delta_a^2\right]^2}. \tag{8}$$

The validity of the analytical expression is illustrated in Fig. 2. The exponential cooling behavior is well captured in the regime where the Doppler shift is small compared to the emitter detuning. In the optimal regime, an additional effect of power broadening has to be taken into account limiting the applicable laser drive strength and an optimal detuning Δ_a close to the value of γ emerges. For smaller decay rates and some fixed $\Delta_a \gg \gamma$ the expression above instead shows a linear scaling with γ. This is the premise for using an optical cavity to enhance the rate of spontaneous emission and subsequently improve the cooling rate.

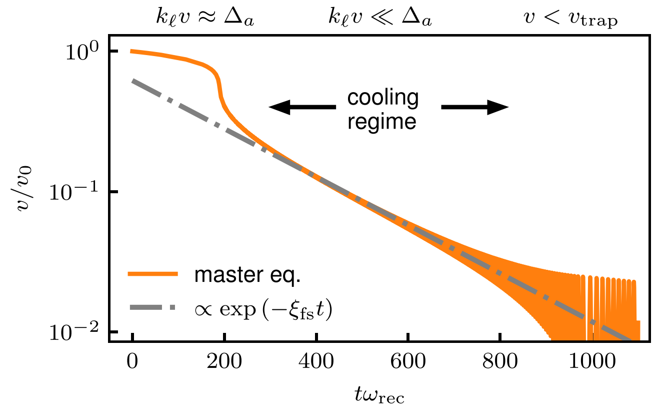

FIG. 2. Illustration of different cooling regimes obtained from numerical simulation of the master equation for a particle initially exhibiting a large Doppler shift. Within the regime of validity of the small shift approximation $k_\ell v \ll \Delta_a$, the exponential decay is well captured by the theoretical analysis. Finally, when the kinetic energy of the emitter is lower than the potential energy at a maximum of the standing wave ($v < v_{\mathrm{trap}}$), the emitter gets trapped around a potential minimum and starts oscillating around it. Parameters in units of γ: $\Omega = 1$, $\Delta_a = 10$, $\omega_{\mathrm{rec}} = 0.5$, $k_\ell v_0 = 18$.

B. Purcell-modified Doppler cooling of a closed transition system

Let us now assume that the two-level system is positioned inside an optical cavity and coupled to the spatially confined light field via the position-dependent light-matter coupling $g(x) = g\cos(k_c x)$, where k_c (corresponding frequency ω_c) is the wave vector of the cavity mode and g quantifies the maximum coupling at an antinode of the optical mode. For a two-level transition $g = d_{eg}\sqrt{\omega_c/(2\varepsilon_0 V)}$ where V is the optical mode volume. Furthermore, the cavity is driven with an amplitude η and frequency ω_ℓ. The description of the single-mode cavity is performed in terms of the bosonic annihilation operator $\hat{a}$ satisfying $[\hat{a}, \hat{a}^\dagger] = 1$. The time-independent Hamiltonian (in a frame rotating at ω_ℓ) is given by

$$\hat{\mathcal{H}} = \hat{\mathcal{H}}_0 + \hbar\Delta_c\hat{a}^\dagger\hat{a} + \mathrm{i}\hbar\eta[\hat{a} - \hat{a}^\dagger] + \hbar g(\hat{x})[\hat{\sigma}^\dagger\hat{a} + \hat{\sigma}\hat{a}^\dagger], \tag{9}$$

where $\Delta_c = \omega_c - \omega_\ell$ is the cavity detuning and the last two terms are the cavity drive and the light-matter coupling according to the Jaynes-Cummings model. Loss from the cavity at rate κ is described by the Lindblad superoperator

$$\mathcal{L}_c[\hat{\rho}] = \kappa[2\hat{a}\hat{\rho}\hat{a}^\dagger - \hat{a}^\dagger\hat{a}\hat{\rho} - \hat{\rho}\hat{a}^\dagger\hat{a}]. \tag{10}$$

We assume low excitation and factorizations of expectation values as in Eqs. (4). Additionally, we factorize light and matter expectation values $\langle\hat{a}\hat{\sigma}\rangle = \langle\hat{a}\rangle\langle\hat{\sigma}\rangle$, with the notation $\alpha = \langle\hat{a}\rangle$. Under these assumptions, we derive the following equations of motion:

$$\dot{\alpha} = -(\kappa + \mathrm{i}\Delta_c)\alpha - \mathrm{i}g(x)\beta - \eta, \tag{11a}$$

$$\dot{\beta} = -(\gamma + \mathrm{i}\Delta_a)\beta - \mathrm{i}g(x)\alpha, \tag{11b}$$

$$\dot{p} = -\hbar g'(x)(\beta\alpha^* + \beta^*\alpha), \tag{11c}$$

$$\dot{x} = p/m. \tag{11d}$$

The equations of motion in Eqs. (11) are a set of coupled nonlinear differential equations, such that already for a single particle a general analytical solution is nontrivial, if not impossible. However, from the physical problem considered (Doppler cooling in the Purcell regime) a clear hierarchy of timescales for the different degrees of freedom emerges, enabling an analytical treatment. The Purcell regime is characterized by large cavity losses $\kappa \gg (g, \gamma)$, such that the cavity field evolves on the shortest timescale. Furthermore, as we are interested in the Doppler cooling process, where the upper bound of the cooling rate is the recoil frequency $\omega_{\rm rec}$, the change in velocity corresponds to the longest timescale. We therefore start by eliminating the cavity field, proceed by determining the emitter coherence, and at last solve the motion of the emitter. Formal integration of the equation of motion for the cavity mode α to first order in g/κ gives (details in Appendix A 1)

$$\alpha = -\frac{\eta}{\kappa + \mathrm{i}\Delta_c} - \frac{\mathrm{i}g(x)\beta}{\kappa + \mathrm{i}\delta}, \tag{12}$$

with $\delta = \omega_0 - \omega_c$, the emitter-cavity detuning. We now see that the cavity field consists of two contributions, first the response to the direct drive and second the induced field of the emitter. The first term in Eq. (12) leads to the same dynamics as in the free space, i.e., a spatially dependent drive of the emitter coherence. The second term is therefore the crucial one, resulting in an effective cavity-mediated self-interaction of the emitter. The Floquet expansion of β now leads to a system of equations for the Floquet coefficients b_n of the form

$$b_n[\gamma + \mathrm{i}(\Delta_a + \mathrm{i}nk_c v)] + \frac{g^2}{4\kappa}(b_{n+2} + b_{n-2} + 2b_n) = -\frac{\mathrm{i}\Omega}{2}(\delta_{n,+1} + \delta_{n,-1}) \tag{13}$$

for the cavity resonant with the atom $\delta = 0$ and the drive $\Omega = -g\eta/(\kappa + \mathrm{i}\Delta_c)$. The cavity couples all odd Floquet coefficients b_n since only the coefficients $b_{\pm 1}$ are directly driven and only coefficients with an index separated by ± 2 are coupled. The physical interpretation is the following. The cavity mode is driven with constant amplitude (in the rotating frame) and couples to the emitter via light-matter coupling with a standing wave spatial profile. Due to the nonzero velocity of the emitter any exchange of excitation between emitter and cavity results in a shift in frequency by the Doppler shift $\pm k_c v$. Elimination of the cavity field then results in an effective description where the emitter is directly driven with frequency components $\pm k_c v$ and an effective coupling between the frequency components separated by $\pm 2k_c v$ is obtained. The coupling corresponds to processes where a photon is emitted and then reabsorbed, such that the total Doppler shift either adds $\pm k_c v \pm k_c v = \pm 2k_c v$, resulting in the coupling between b_n and $b_{n\pm 2}$ or cancels $\pm k_c v \mp k_c v = 0$, resulting in a modification of b_n. The equations for the Floquet coefficients given by Eq. (13) can be cast into a matrix form with tridiagonal shape with constant sub and superdiagonal elements and nonconstant diagonal. In principle, the equations can be solved up to any order. However, we find that a reduction to a two-dimensional subspace involving only components $b_{\pm 1}$ suffices for $\mathcal{C}\gamma/\Delta_a \ll 1$ and allows for the derivation of simple scaling laws of the cooling rate. An approach to include all b_n is sketched in Appendix A 1. We obtain the free-space case given by Eq. (5) from Eq. (13) by fixing the drive Ω and let $g^2/\kappa \to 0$.

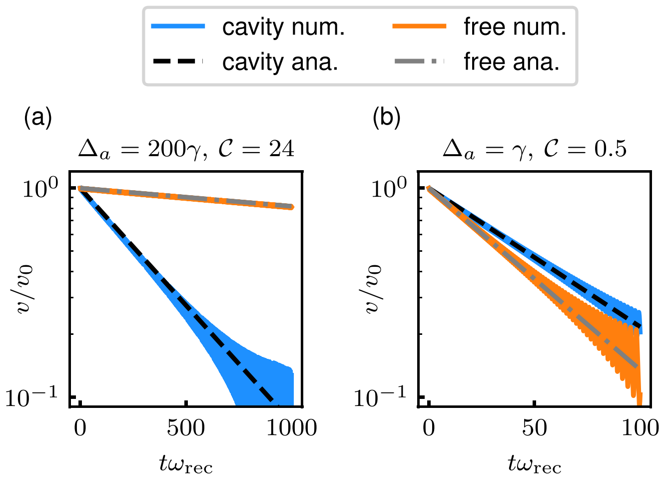

FIG. 3. Comparison between the numerical simulation of the emitter velocity obtained from the mean-field equations inside the cavity to free space, which confirms the scaling of the cooling rate in Eq. (15). (a) For large detuning $\Delta_a \gg \gamma(1 + \mathcal{C})$ the cooling rate ξ_c is enhanced compared to free space and scales linearly with the cooperativity. (b) For $\Delta_a = \gamma$ the cooling rate is reduced inside the cavity compared to free space. Parameters in units of γ for (a) $g = 155$, $\kappa = 1000$, $\Delta_a = \Delta_c = 200$, $\eta \approx 132$, $\omega_{\rm rec} = 2.5$, $k_c v_0 = 30$ and for (b) $g = \sqrt{500}$, $\kappa = 1000$, $\Delta_a = \Delta_c = 1$, $\eta \approx 6$, $\omega_{\rm rec} = 0.02$, $k_c v_0 = 0.15$. Note the large difference in $\omega_{\rm rec}$ for the two cases.

Solving the reduced two-dimensional system leads to the following coefficients:

$$b_{\pm 1} = -\frac{\mathrm{i}\Omega}{2}\frac{1}{\gamma(1 + \mathcal{C}/4) + \mathrm{i}(\Delta_a \pm k_c v)} \times \left[1 + \frac{g^2}{4\kappa}\sum_{\pm}\frac{1}{\gamma(1 + \mathcal{C}/4) + \mathrm{i}(\Delta_a \pm k_c v)}\right]^{-1}. \tag{14}$$

Just as in free space we only keep terms in the equation of motion for the momentum which do not oscillate spatially, as the oscillating terms average to zero. Expanding Eq. (14) to first order in $k_c v/\Delta_a$ yields the cavity modified cooling rate

$$\xi_c = \frac{4|\Omega|^2\omega_{\rm rec}\Delta_a\gamma(1 + \mathcal{C}/2)}{[\Delta_a^2 + \gamma^2(1 + \mathcal{C}/4)^2][\Delta_a^2 + \gamma^2(1 + 3\mathcal{C}/4)^2]}. \tag{15}$$

For large detuning $\Delta_a \gg \gamma(1 + \mathcal{C})$ an expected linear increase in the cooling rate stemming from the Purcell-modified emission rate is obtained. We test this result against numerical simulation of the mean-field equations in Fig. 3(a) where an increase by a factor of $1 + \mathcal{C}/2$ in the cooling rate is observed. However, the improvement with $\mathcal{C}$ only holds in the regime $\Delta_a \gg \gamma(1 + \mathcal{C})$ which is suboptimal, but might be relevant for faster particles where the large Doppler shift requires higher detunings to allow for their capture, as $k_c v \gg \gamma$. In the regime $\Delta_a = \gamma$ the cooling rate decreases with increasing cooperativity, which is confirmed with numerics in Fig. 3(b) for small cooperativity where our analytical approach is valid.

C. Free-space Doppler cooling of a nonclosed transition system

We now consider a Λ-type three-level system, as displayed in Fig. 1(c) in free space. We assume that the drive couples solely to the transition between the ground state $|g\rangle$ and the excited state $|e\rangle$. Spontaneous emission, however, takes place between both excited state $|e\rangle$ and ground state $|g\rangle$ at rate γ and excited state $|e\rangle$ and intermediate state $|i\rangle$ at rate γ'. One could, in principle, assume an additional mechanism for population transfer from the intermediate state to the ground state at rate Γ. For molecules in a gas phase, this could correspond to population trapping in the rovibrational manifold and the value of Γ could be negligible (and we therefore neglect it in the following). This results in population trapping in the intermediate level and subsequently an effective loss of population from the cooling cycle. Since the intermediate state only couples via spontaneous emission from the excited state the Hamiltonian in Eq. (3) is unchanged and we merely include an additional Lindblad superoperator with collapse operator $\hat{\sigma}' = |i\rangle\langle e|$ at rate γ'. The corresponding mean-field equations including the populations of ground state n_g, excited state n_e, and intermediate state n_i read

$$\dot{\beta} = -(\gamma + \gamma' + \mathrm{i}\Delta_a)\beta - \mathrm{i}\Omega(x)[n_g - n_e], \tag{16a}$$

$$\dot{n}_g = 2\gamma n_e - \mathrm{i}\Omega(x)[\beta - \beta^*], \tag{16b}$$

$$\dot{n}_e = -2(\gamma + \gamma')n_e + \mathrm{i}\Omega(x)[\beta - \beta^*], \tag{16c}$$

$$\dot{n}_i = 2\gamma' n_e, \tag{16d}$$

$$\dot{p} = -\hbar\Omega'(x)[\beta + \beta^*], \tag{16e}$$

$$\dot{x} = p/m. \tag{16f}$$

In such a case, the system of equations are very similar to the ones for the closed transition system with the difference that the drive of the emitter coherence β has a term proportional to n_g for $n_e \ll n_g$. This simply suggests that the cooling rate for the nonclosed system is similar to the closed system case, with the distinction that it has an additional dependence on n_g such that it subsequently gets reduced to zero in time as population is lost to the intermediate state. We now solve Eqs. (16) under the assumption of low excitation $n_e \ll n_g$. Therefore, we can assume that the populations evolve much slower than the emitter coherence ($\dot{n}_g \ll \gamma + \gamma'$), such that we can directly solve Eq. (16a) in a similar fashion as already sketched out in the previous subsection. The Floquet coefficients of the emitter coherence now have a slow time dependence via the time-dependent ground-state population. Under the assumption of steady state for the excited-state population we obtain for the ground-state population

$$\dot{n}_g = -\frac{\gamma'\Omega^2}{\Delta_a^2 + \gamma_{\mathrm{tot}}^2} n_g = -\mu_{\mathrm{fs}} n_g, \tag{17}$$

where we define the total spontaneous decay rate $\gamma_{\mathrm{tot}} = \gamma + \gamma'$. The effective loss rate in Eq. (17) is simply the excitation probability times the rate of spontaneous emission into the intermediate state. The time-dependent ground-state population, which approaches 0 for $t \to \infty$, results in a time-dependent cooling rate of the form

$$\dot{v} = -\xi_{\mathrm{fs}} n_g(t) v = -\xi_{\mathrm{fs}} \mathrm{e}^{-\mu_{\mathrm{fs}} t} v, \tag{18}$$

with the solution

$$v(t) = v_0 \exp\left[\frac{\xi_{\mathrm{fs}}}{\mu_{\mathrm{fs}}}(\mathrm{e}^{-\mu_{\mathrm{fs}} t} - 1)\right], \tag{19}$$

where ξ_{fs} has the same form as in Eq. (8) but with γ replaced by γ_{tot}. For $t \to \infty$ when all population is lost to the intermediate state the final velocity is given by

$$v_{\mathrm{fs,final}} = v_0 \exp\left(-\frac{\xi_{\mathrm{fs}}}{\mu_{\mathrm{fs}}}\right) = v_0 \exp\left[-\frac{4\omega_{\mathrm{rec}}\gamma_{\mathrm{tot}}\Delta_a}{\gamma'\left(\Delta_a^2 + \gamma_{\mathrm{tot}}^2\right)}\right]. \tag{20}$$

The lowest final velocity is reached for $\Delta_a = \gamma_{\mathrm{tot}}$. In the regime $\Delta_a \gg \gamma_{\mathrm{tot}}$ the final velocity scales exponentially with the spontaneous decay rate γ_{tot}.

D. Purcell-modified Doppler cooling of a nonclosed transition system

We continue with the nonclosed transition system, now inside a cavity. The mean-field equations of motion derived from the Hamiltonian in Eq. (9) including populations and the spontaneous emission rates indicated in Fig. 1(c) read

$$\dot{\alpha} = -(\kappa + \mathrm{i}\Delta_c)\alpha - \mathrm{i}g(x)\beta - \eta, \tag{21a}$$

$$\dot{\beta} = -(\gamma + \gamma' + \mathrm{i}\Delta_a)\beta - \mathrm{i}g(x)\alpha[n_g - n_e], \tag{21b}$$

$$\dot{n}_g = 2\gamma n_e - \mathrm{i}g(x)[\beta\alpha^* - \beta^*\alpha], \tag{21c}$$

$$\dot{n}_e = -2(\gamma + \gamma')n_e + \mathrm{i}g(x)[\beta\alpha^* - \beta^*\alpha], \tag{21d}$$

$$\dot{n}_i = 2\gamma' n_e, \tag{21e}$$

$$\dot{p} = -\hbar g'(x)[\beta\alpha^* + \beta^*\alpha], \tag{21f}$$

$$\dot{x} = p/m. \tag{21g}$$

Again the equations of motion for the nonclosed system closely resemble the closed transition system, but with time-dependent populations. With the populations evolving much slower than the emitter coherence and the cavity, we can again utilize our solution for the closed transition system in terms of the Floquet coefficients which are now time dependent via the ground-state population. The population dynamics of the ground state are then dictated by the equation

$$\dot{n}_g = -\frac{\gamma'|\Omega|^2}{\gamma_{\mathrm{tot}}^2(1 + 3\mathcal{C}n_g/4)^2 + \Delta_a^2} n_g, \tag{22}$$

where we define the cooperativity as $\mathcal{C} = g^2/(\kappa\gamma_{\mathrm{tot}})$. Let us now distinguish two regimes: (i) $\gamma_{\mathrm{tot}}\mathcal{C}/(4\Delta_a) \ll 1$, in which case the reduced two-dimensional description of the Floquet coefficients suffices and analytical results are tractable and (ii) $\gamma_{\mathrm{tot}}\mathcal{C}/(4\Delta_a) \geqslant 1$, in which case many Floquet coefficients have to be taken into account. An approach to include Floquet coefficients to arbitrary order is sketched in Appendix A 2. In regime (i), for sufficiently large Δ_a, Eq. (22) becomes equivalent to Eq. (17), such that the time evolution of the ground state is not modified by the cavity. This is confirmed with numerics in Fig. 4(b). Furthermore, the cooling rate scales linearly with the cooperativity in this regime. The reduction of ground-state population $n_g(t) = \exp(-\mu_{\mathrm{fs}} t)$ will then lead

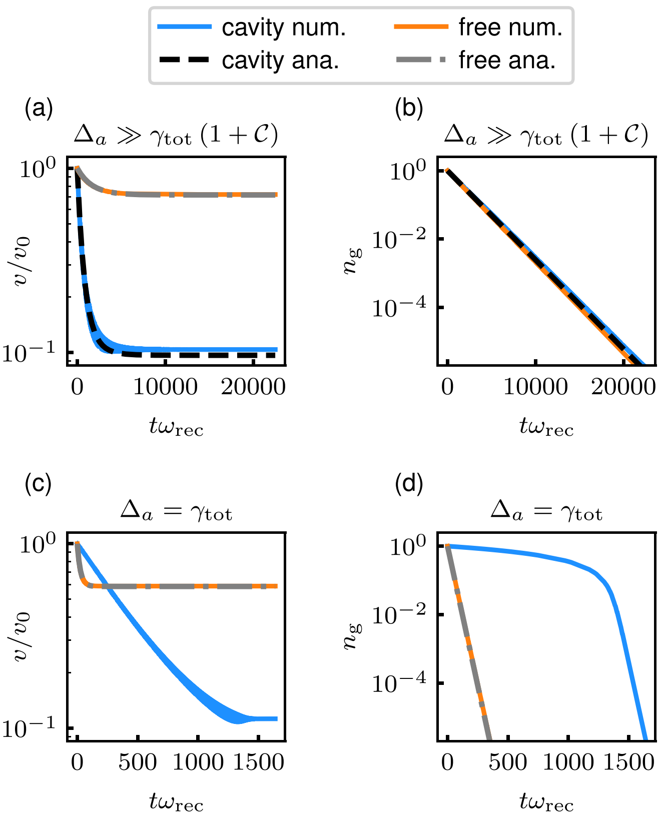

FIG. 4. Time evolution of (a) velocity and (b) ground-state population in regime (i) $\gamma_{\rm tot}\mathcal{C}/(4\Delta_a) \ll 1$ with $\Delta_a = 200\gamma_{\rm tot}$ and $\mathcal{C} = 24$. (a) Due to the Purcell-enhanced cooling rate in the strong detuned regime the final velocity is now reduced. (b) The loss of population to the intermediate state shows no Purcell modification in regime (i), as expected from Eq. (22). Time evolution of (c) velocity and (d) ground-state population in regime (ii) $\gamma_{\rm tot}\mathcal{C}/(4\Delta_a) \gg 1$ with $\Delta_a = \gamma_{\rm tot}$ and $\mathcal{C} = 24$. (c) The cooling rate inside the cavity is decreased compared to free space, but due to the reduced loss of population (d), the final velocity is still reduced. Numerical parameters for (a), (b) in units of $\gamma_{\rm tot}$: $\gamma = 0.85$, $g = 155$, $\kappa = 1000$, $\Delta_a = \Delta_c = 200$, $\eta \approx 132$, $\omega_{\rm rec} = 2.5$, $k_c v_0 = 30$ and for (c), (d): $\gamma = 0.85$, $g = 155$, $\kappa = 1000$, $\Delta_c = \Delta_a = 1$, $\eta \approx 0.9$, $\omega_{\rm rec} = 0.04$, $k_c v_0 = 0.15$. The performance in the different regimes is only similar due to the large difference in $\omega_{\rm rec}$.

to an exponential reduction in the cooling rate and an exponential reduction of the Purcell modification of the cooling rate with rate $2\mu_{\rm fs}$ [see Eq. (23)]. We can explicitly write the equation of motion for the velocity as

$$\dot{v} = -\xi_c(t)v = -\xi_{\rm fs}\left[n_g(t) + \frac{\mathcal{C}}{2}n_g^2(t)\right]v, \qquad (23)$$

with the following solution:

$$v = v_0 \exp\left\{\frac{\xi_{\rm fs}}{\mu_{\rm fs}}\left[(\mathrm{e}^{-\mu_{\rm fs}t} - 1) + \frac{\mathcal{C}}{4}(\mathrm{e}^{-2\mu_{\rm fs}t} - 1)\right]\right\}. \qquad (24)$$

We check the validity of Eq. (24) against the numerics in Fig. 4(a). The final velocity reached inside the cavity is then reduced due to the Purcell-enhanced cooling rate, while the loss of population is not modified. The performance of the Purcell-modified cooling mechanism compared to free space can then be quantified by the ratio of the final velocities when all population is lost to the intermediate state

$$\frac{v_{\rm c,final}}{v_{\rm fs,final}} = \exp\left(-\frac{\xi_{\rm fs}}{\mu_{\rm fs}}\frac{\mathcal{C}}{4}\right). \qquad (25)$$

In the regime (ii) $\mathcal{C}\gamma_{\rm tot}/\Delta_a \gg 1$ we show only numerical results of the dynamics [see Figs. 4(c) and 4(d)], as the restriction to the Floquet coefficients $b_{\pm 1}$ is no longer valid. The loss of population to the intermediate state is now reduced by the Purcell effect inside the cavity, departing from the purely exponential decay [see Fig. 4(d)]. We see in Fig. 4(c) that the cooling rate inside the cavity is reduced compared to free space, as expected from the cooling rate for the closed transition system in Eq. (15). However, due to the reduction in population loss, the cooling time is increased and therefore a lower final velocity is reached, despite the reduced cooling rate. We have now identified two mechanisms by which the cavity can enhance the cooling process of a nonclosed transition system, i.e., increase the amount of removed kinetic energy. First, an increase in the cooling rate which appears in the regime $\Delta_a \gg \gamma_{\rm tot}(1+\mathcal{C})$, where the population dynamics are not modified by the cavity. Second, a decrease in the loss of population from the cooling cycle which appears most prominently in the regime $\Delta_a \approx \gamma_{\rm tot}$, where the cooling rate is reduced.

To understand how the effects of the cavity on cooling rate and population loss compete, we derive an analytical result for the final velocity, in regime (i) $\gamma_{\rm tot}\mathcal{C}/(4\Delta_a) \ll 1$, but now considering the Purcell modification of the dynamics of the ground-state population given by Eq. (22). The derivation, detailed in Appendix A 2, indicates that $v(t\to\infty) = v_0 \exp\{-\int_0^\infty \xi[n_g(t)]dt\}$, where the exponent is approximated to first order in $\mathcal{C}\gamma_{\rm tot}/\Delta_a$ by

$$\int_0^\infty \xi_{\rm c}[n_g(t)]dt \approx \frac{\xi_{\rm fs}}{\mu_{\rm fs}}\left[1 + \frac{\mathcal{C}\Delta_a^2}{4(\gamma_{\rm tot}^2 + \Delta_a^2)}\right]. \qquad (26)$$

Therefore, already in regime (i) $\gamma_{\rm tot}\mathcal{C}/(4\Delta_a) \ll 1$ we see the onset of the behavior observed in Figs. 4(c) and 4(d), where the reduction of population loss at the expense of a reduced cooling rate leads to a reduction in the final velocity. This behavior differs from free space, where an increase in the rate of spontaneous emission is expected to reduce the final velocity for $\Delta_a = \gamma_{\rm tot}$ [see Eq. (20)]. Furthermore, Eq. (26) indicates that the lowest final velocity relative to free space is obtained for $\Delta_a = \gamma_{\rm tot}$, i.e., in the regime where the cooling rate is reduced. We perform numerical simulations of the final velocity beyond the validity of the analytical results (see Fig. 5), which show that the lowest final velocity is indeed obtained for $\Delta_a \approx \gamma_{\rm tot}$.

III. MANY-PARTICLE COOLING INSIDE OPTICAL CAVITIES

Let us now consider the case of $\mathcal{N}$ particles inside an optical cavity, where the single-particle cooperativity is small

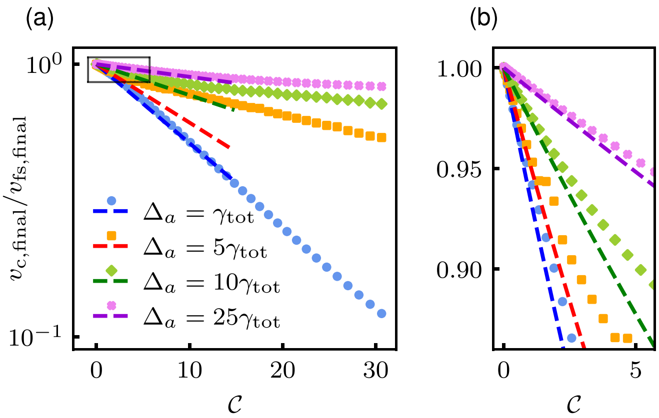

FIG. 5. (a) Performance of the cooling of a single nonclosed transition system inside the cavity compared to free space as a function of the cooperativity. The dashed lines correspond to the analytical scaling in Eq. (26) and the markers are obtained from numerical simulation of the mean-field equations. In (b) we show the rectangle marked in (a) for small cooperativity. For regime (i) $\mathcal{C}\gamma_{\mathrm{tot}}/\Delta_a \ll 1$ the scaling with the cooperativity given by Eq. (26) is confirmed. However, for large cooperativity the scaling of the final velocity with the cooperativity is generally lower than expected, but still, the final velocity remains reduced. Numerical parameters in units of γ_{tot}: $\gamma = 0.85$, $\kappa = 1000$, $\Delta_c = \Delta_a$, $\eta = \sqrt{0.01(\Delta_a^2 + \gamma_{\mathrm{tot}}^2)(\kappa^2 + \Delta_c^2)/g^2}$, $\omega_{\mathrm{rec}} = 0.04$, $k_c v_0 = 0.2\Delta_a$.

$\mathcal{C} \ll 1$ but the collective cooperativity is large $\mathcal{N}\mathcal{C} \gg 1$. The aim is to elucidate whether the large collective cooperativity $\mathcal{C}\mathcal{N}$ can influence the cooling dynamics of an individual emitter or whether it is solely the single-particle cooperativity $\mathcal{C}$ which is relevant for cooling.

A. Purcell-modified Doppler cooling of $\mathcal{N}$ closed transition systems

The total Hamiltonian for a set of $\mathcal{N}$ identical particles is the direct extension of the Hamiltonian of Eq. (9) where we now sum over the particle index $j = 1, \dots, \mathcal{N}$. Similarly to the procedure in the previous section, we derive the set of coupled equations for the factorized expectation values in the low excitation regime

$$\dot{\alpha} = -(\kappa + \mathrm{i}\Delta_c)\alpha - \mathrm{i}\sum_{j=1}^{\mathcal{N}} g(x_j)\beta_j - \eta, \tag{27a}$$

$$\dot{\beta}_j = -(\gamma + \mathrm{i}\Delta_a)\beta_j - \mathrm{i}g(x_j)\alpha, \tag{27b}$$

$$\dot{p}_j = -\hbar g'(x_j)[\beta_j\alpha^* + \beta_j^*\alpha], \tag{27c}$$

$$\dot{x}_j = p_j/m. \tag{27d}$$

We proceed by performing a formal integration of the cavity mode in first order in g/κ to yield the $\mathcal{N}$ emitter equivalent of Eq. (12). In addition, each particle coherence is expanded in the harmonics of the cavity field $\beta_j = \sum_{n=-\infty}^{\infty} b_{j,n}\mathrm{e}^{\mathrm{i}nk_c x_j}$ (see Appendix B2). This now gives a system of equations where all Floquet coefficients $b_{j,n}$ are coupled, where we again truncate to $b_{j,\pm 1}$ as in Sec. II B. The coupling is explicitly given by

$$\begin{pmatrix} a_{1,-} & 1 & \dots & \dots & 1 & 1 \\ 1 & \ddots & \ddots & & & 1 \\ \vdots & 1 & a_{\mathcal{N},-} & 1 & & \vdots \\ \vdots & & 1 & a_{1,+} & 1 & \vdots \\ 1 & & & \ddots & \ddots & 1 \\ 1 & 1 & \dots & \dots & 1 & a_{\mathcal{N},+} \end{pmatrix} \begin{pmatrix} b_{1,-} \\ \vdots \\ b_{\mathcal{N},-} \\ b_{1,+} \\ \vdots \\ b_{\mathcal{N},+} \end{pmatrix} = -\frac{2\mathrm{i}\kappa\Omega}{g^2}\begin{pmatrix} 1 \\ \vdots \\ 1 \\ 1 \\ \vdots \\ 1 \end{pmatrix}, \tag{28}$$

with $a_{j,\pm} = [\gamma + \mathrm{i}(\Delta_a \pm k_c v_j)]4\kappa/g^2 + 2$. The matrix can be inverted using the Sherman-Morrison formula [30], yielding the following coefficients:

$$b_{j,\pm 1} = -\frac{\mathrm{i}\Omega}{2}\frac{1}{[\gamma(1+\mathcal{C}/4) + \mathrm{i}(\Delta_a \pm k_c v_j)]} \times \left[1 + \frac{g^2}{4\kappa}\sum_{m,\pm}^{\mathcal{N}}\frac{1}{[\gamma(1+\mathcal{C}/4) + \mathrm{i}(\Delta_a \pm k_c v_m)]}\right]^{-1}. \tag{29}$$

The Floquet coefficient $b_{j,\pm 1}$ depends on all velocities v_m, which leads to a coupling of the equations of motion for all emitters. However, $b_{j,\pm}$ is an even function in all velocities $v_{m\neq j}$, whereas it has both even and odd parts in v_j. Therefore, a Taylor expansion up to first order in $k_c v_m/\Delta_a$ removes the dependency of $b_{j,\pm 1}$ on all velocities v_m with $m \neq j$, resulting in a diagonal equations of motion for the velocities. The physical interpretation is illustrated in Fig. 6(c). Truncating the Floquet coefficients $b_{j,n}$ to $n = \pm 1$ corresponds to the black rectangle in Fig. 6(c). Under this approximation a contribution to coefficient $b_{j,-1}$ is obtained from every coefficient $b_{i,\pm 1}$, as indicated by the black arrows. This corresponds to processes where a photon is either directly absorbed by the emitter from the cavity, or the photon is absorbed by an emitter, reemitted into the cavity, and then absorbed again. As the Doppler shift from absorption and reemission in our approximation cancels, the coefficient $b_{j,-1}$ only depends on $-k_c v_j$. We can thus write

$$b_{j,\pm 1} \approx b^{(0)} \pm k_c v_j b^{(1)}, \tag{30}$$

where we defer the explicit expression to Appendix B 1 Eq. (B4). With Eq. (30) we determine β_j and therefore also α. We obtain for α

$$\alpha = -\frac{\eta}{\kappa + \mathrm{i}\Delta_c} - \frac{\mathrm{i}g}{\kappa}\mathcal{N}b^{(0)}, \tag{31}$$

where we omitted terms which oscillate with the Doppler frequency. Collective effects appear both in $b_{j,\pm 1}$, see Eq. (29), and in α, see Eq. (31). We obtain the cooling rate

$$\xi_c = \frac{4|\Omega|^2\omega_{\mathrm{rec}}\Delta_a\gamma(1+\mathcal{C}/2)}{[\gamma^2(1+\mathcal{C}/4)^2 + \Delta_a^2]\{\gamma^2[1+\mathcal{C}(2\mathcal{N}+1)/4]^2 + \Delta_a^2\}}. \tag{32}$$

The collective cooperativity $\mathcal{C}\mathcal{N}$ only appears in the denominator of the cooling rate ξ_c, which implies worse cooling for increased collective cooperativity and hence particle number. The effects which lead to the form of ξ_c in Eq. (32) are schematically represented in Fig. 6. The cavity field drives

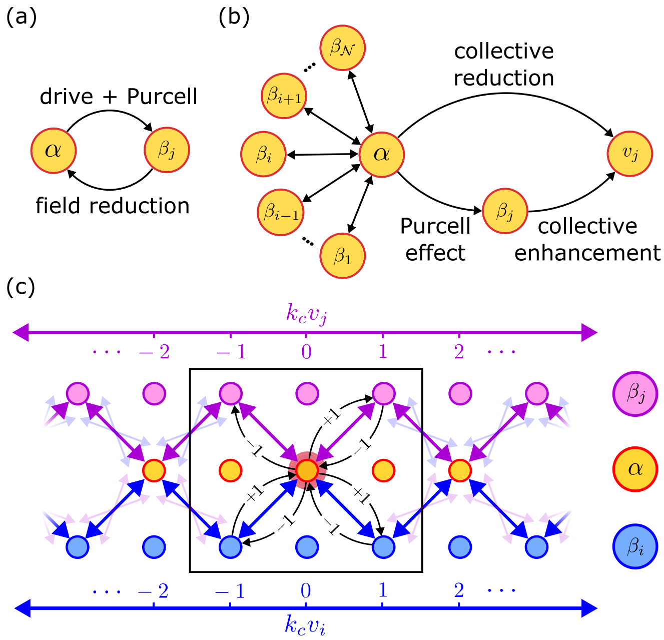

FIG. 6. (a) The cavity mode drives each emitter, i.e., induces a dipole moment and provides an additional decay channel (Purcell effect). The induced dipole moment of each emitter in turn reduces the amplitude of the cavity field. (b) The velocity of particle j evolves according to the interaction of its coherence with the cavity field [see Eq. (27c)]. The collective modification of the emitter coherence β_j leads to a collective enhancement of the emitter decay rate [see Eq. (29)]. However, due to the collective reduction of the cavity field by the emitters [see Eq. (31)], an increase in the amount of emitters always leads to a reduced cooling rate [see Eq. (32)]. (c) Illustration of the coupling between different Floquet coefficients, as described in the main text. On the single-particle level the exchange of a photon between the emitter and the cavity results in a frequency shift $\pm k_c v$, depending on whether the photon is absorbed from or emitted to the left or right. This is indicated by the solid coloured arrows. For many particles this results in a coupling between the Floquet coefficients of different particles. The black arrows indicate the contribution to $b_{j,-1}$ from $b_{j,+1}, b_{i,\pm 1}$. In the many-emitter case coupling to Floquet coefficients $b_{j,n}$ with $|n| > 1$, results in the generation of noninteger frequency components $k_c(nv_j + mv_i)$, as $v_i \neq v_j$, indicated by the translucent arrows.

each emitter coherence and provides an additional decay channel. In turn, the field generated by the emitters reduces the cavity field, such that the force component on particle j obtained from the interaction with the field generated by particle i with $i \neq j$ effectively corresponds to heating rather than cooling.

B. Purcell-modified Doppler cooling of $\mathcal{N}$ nonclosed transition systems

We now extend the results for $\mathcal{N}$ closed transition systems inside a cavity to $\mathcal{N}$ nonclosed transition systems and again derive the equations of motion for the factorized expectation values. As for the single nonclosed transition system we include the equations of motion for the populations, such that we obtain

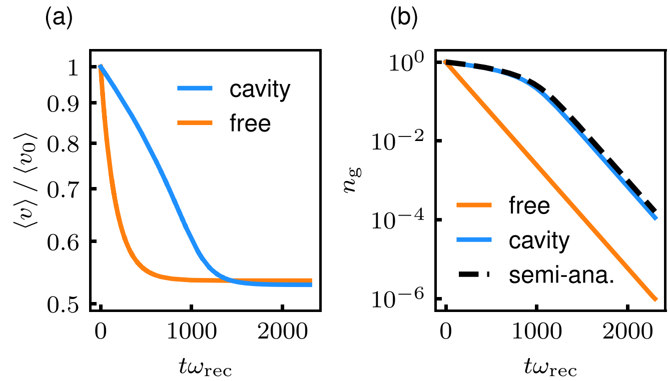

FIG. 7. (a) Numerical simulation of the mean-field equations for $\mathcal{N} = 400$ nonclosed transition emitters with $\mathcal{C} = 0.15$ and $\mathcal{C}\mathcal{N} = 60$. The initial velocity distribution is Gaussian while the initial position distribution is uniform over $2\pi/k_c$. Despite the collective reduction of the cooling rate, as obtained from Eq. (32), the final velocity reached inside the cavity is almost identical to free space, as the cavity inhibits population migration from the cooling cycle. However, the reduction in the final velocity is only a single-particle effect $\propto \mathcal{C}$ with $\mathcal{C} \ll 1$, as derived in Eq. (35). The scale on the y axis is logarithmic. (b) Collective Purcell inhibition of population loss showing departure from the exponential dynamics in free space. The semi-analytical curve is a numerical simulation of Eq. (34). Numerical parameters normalized to $\gamma_{\rm tot}$: $\gamma = 0.7$, $g = 7.5$, $\eta = 50$, $\Delta_a = \Delta_c = 10$, $\kappa = 375$, $\omega_{\rm rec} = 0.5$, $k_c\langle v_0\rangle = 1.5$, $\sqrt{k_c^2(\langle v_0^2\rangle - \langle v_0\rangle^2)} = 0.1$.

$$\dot{\alpha} = -(\kappa + \mathrm{i}\Delta_c)\alpha - \mathrm{i}\sum_{m=1}^{\mathcal{N}} g(x_m)\beta_m - \eta, \tag{33a}$$

$$\dot{\beta}_j = -(\gamma + \gamma' + \mathrm{i}\Delta_a)\beta_j - \mathrm{i}g(x_j)\alpha[n_{j,g} - n_{j,e}], \tag{33b}$$

$$\dot{n}_{j,g} = 2\gamma n_{j,e} - \mathrm{i}g(x_j)[\beta_j\alpha^* - \beta_j^*\alpha], \tag{33c}$$

$$\dot{n}_{j,e} = -2(\gamma + \gamma')n_{j,e} + \mathrm{i}g(x_j)[\beta_j\alpha^* - \beta_j^*\alpha], \tag{33d}$$

$$\dot{n}_{j,i} = 2\gamma' n_{j,e}, \tag{33e}$$

$$\dot{p}_j = -\hbar g'(x_j)[\beta_j\alpha^* + \beta_j^*\alpha], \tag{33f}$$

$$\dot{x}_j = p_j/m. \tag{33g}$$

Again we follow the steps outlined in Sec. II D to derive a differential equation for the ground-state population

$$\dot{n}_g = -\frac{\gamma'|\Omega|^2}{\gamma_{\rm tot}^2[1 + (2\mathcal{N} + 1)\mathcal{C}n_g/4]^2 + \Delta_a^2} n_g, \tag{34}$$

where we dropped the particle index since the population transfer is position and velocity independent within our approximations and therefore identical for each particle. Numerical simulation of this equation shows agreement with the simulation of the full mean-field equations, as illustrated in Fig. 7(b). The reduced population loss, as already derived for a single particle in Eq. (22) shows now a dependence on the collective cooperativity $\mathcal{C}\mathcal{N}$, instead of the single-particle cooperativity $\mathcal{C}$, i.e., it hints towards the possibility of a collective Purcell enhancement. A full analytical solution of the dynamics remains intractable. However, we can again find an exact expression within our approximations for the final velocity, as already for the single nonclosed transition system (details in Appendix B 2). Here, we give the expression in leading order in the single-particle cooperativity

$$v_{\mathrm{c,final}} = \exp\left[-\frac{\xi_{\mathrm{fs}}}{\mu_{\mathrm{fs}}}\left(1+\frac{\mathcal{C}\Delta_a^2}{4(\Delta_a^2+\gamma_{\mathrm{tot}}^2)}\right)\right]. \tag{35}$$

The final velocity is independent of the number of emitters $\mathcal{N}$ since the collective effects in the cooling rate in Eq. (32) and population transfer in Eq. (34) cancel, such that only the single-particle effects remain. We confirm this with numerics in Fig. 7(a). Since we have small single-particle cooperativity $\mathcal{C} \ll 1$ the reduction of the final velocity inside the cavity compared to free space is insignificant.

IV. DISCUSSION AND CONCLUSION

We addressed the question of Purcell-modified Doppler cooling of quantum emitters, both with closed and nonclosed electronic transitions. The main effect, at the single-particle level, is the Purcell enhancement of spontaneous emission, which occurs when the cavity losses are high. This can lead to an improvement of cooling rates for both closed and nonclosed transition systems under far detuned conditions. In the regime of optimal cooling the cooling rate is not improved. However, for the nonclosed transition system, the Purcell effect leads to a reduction of population loss, which results in a lower final velocity when all population is lost to the intermediate state. At the level of many closed-transition systems, we show analytically how the cooling rate can be simply computed and find that the collective coupling does not lead to an enhancement of the cooling rate at the individual particle level, rather a collective decrease. For many nonclosed transition systems we show that the final velocity when all population is lost to the intermediate state is independent of the amount of emitters, i.e., shows no collective modification.

An extension of the one-dimensional treatment to three spatial dimensions can be envisioned using our equations by considering configurations of mirrors defining cavity modes in all three dimensions. Alternatively, one can simply reduce the kinetic energy along one direction and provide a thermalization mechanism which would lead to equipartition in all three dimensions.

We can also imagine scenarios where this extra effect of cooling via cavity Purcell enhancement of spontaneous emission could be implemented. For example, microfluidic devices could be integrated with optical cavities, and single molecule-photon coupling with cooperativity of the order of 50 could be reached as in Ref. [24]. For molecules moving in solutions, the cavity effect could enhance the cooling of their ballistic motion. Additionally, we will in the future address the reduction of temperature characterized by diffusive motion by supplementing our equations with classical Brownian noise terms based on a Wiener increment formalism.

ACKNOWLEDGMENTS

We acknowledge fruitful discussions with A. Jaber. We acknowledge financial support from the Max Planck Society. We further acknowledge support by the Deutsche Forschungsgemeinschaft (DFG, German Research Foundation), Project-ID 429529648-TRR 306 QuCoLiMa ("Quantum Cooperativity of Light and Matter"). This work has benefited from state grants managed by the French National Research Agency under the Investments of the Future Program with the Grants No. ANR-21-ESRE-0032 (aQCess), and No. ANR-22-CE47-0013 (CLIMAQS).

APPENDIX A: DOPPLER COOLING OF A SINGLE QUANTUM EMITTER

Let us sketch the procedure we follow to derive the cooling rate for closed and nonclosed transition quantum emitters inside an optical cavity.

1. Single closed transition system inside a cavity

Formal integration of the cavity mode amplitude expectation value from Eqs. (11), assuming free evolution of the emitter coherence β and linearized position $x = vt$, yields

$$\begin{aligned}\alpha &= -\int_0^t \mathrm{i}g[e^{-(\kappa+\mathrm{i}\Delta_c)(t-s)}\cos(k_c vs)\beta(t)e^{-(\gamma+\mathrm{i}\Delta_a)(s-t)}\\ &\qquad + \eta e^{-(\kappa+\mathrm{i}\Delta_c)(t-s)}]ds\\ &= -\mathrm{i}g\beta\sum_{\pm}\left[\frac{1}{2}\frac{e^{\pm\mathrm{i}k_c vt}}{\kappa-\gamma+\mathrm{i}(\delta\pm k_c v)} - \frac{1}{2}\frac{e^{-(\kappa-\gamma+\mathrm{i}(\delta\pm k_c v))t}}{\kappa-\gamma+\mathrm{i}(\delta\pm k_c v)}\right]\\ &\quad - \frac{\eta}{\kappa+\mathrm{i}\Delta_c} + \frac{\eta e^{-(\kappa+\mathrm{i}\Delta_c)t}}{\kappa+\mathrm{i}\Delta_c}\\ &\approx -\frac{\mathrm{i}g(x)\beta}{\kappa+\mathrm{i}\delta} - \frac{\eta}{\kappa+\mathrm{i}\Delta_c},\end{aligned} \tag{A1}$$

with $\delta = \Delta_c - \Delta_a$. Furthermore, we utilized the assumption that $\kappa \gg \gamma, k_c v$ and neglected the transient contributions due to large cavity loss in the Purcell regime. Inserting the final result of Eq. (A1) into the equation of motion for β with the cavity resonant to the emitter $\delta = 0$ and performing a temporal Fourier transform with linearised position $x = vt$ gives a discrete spectrum of the form

$$\begin{aligned}\mathrm{i}\omega\beta(\omega) &= -(\gamma+\mathrm{i}\Delta_a)\beta(\omega)\\ &\quad - \frac{g^2}{4\kappa}[\beta(\omega+2k_c v)+\beta(\omega-2k_c v)+2\beta(\omega)]\\ &\quad - \frac{\mathrm{i}\Omega}{2}[\delta(\omega-k_c v)+\delta(\omega+k_c v)].\end{aligned} \tag{A2}$$

Therefore, the emitter coherence contains only discrete frequencies and leads us to performing a Floquet expansion of the emitter coherence of the form

$$\beta = \sum_{n=-\infty}^{\infty} b_n e^{\mathrm{i}nk_c x}, \tag{A3}$$

which then gives an infinite set of coupled differential equations

$$\begin{aligned}&\dot{b}_n + b_n[\gamma+\mathrm{i}(\Delta_a+nk_c v)] + \frac{g^2}{4\kappa}(b_{n+2}+b_{n-2}+2b_n)\\ &\quad = -\frac{\mathrm{i}\Omega}{2}(\delta_{n,+1}+\delta_{n,-1}).\end{aligned} \tag{A4}$$

We require the solution of β to derive the force acting on the particle. As the emitter velocity evolves much more slowly than the electronic degrees of freedom we may solve the differential equations for the Floquet coefficients b_n in the steady state $\dot{b}_n = 0$. In matrix notation the steady-state solution for the Floquet coefficients takes the form

$$\begin{pmatrix} \ddots & \ddots & \ddots & \ddots & \ddots & & & & & \\ & 0 & c & a_{-3} & c & 0 & & & & \\ \hline & & 0 & c & a_{-1} & c & 0 & & & \\ & & & 0 & c & a_{+1} & c & 0 & & \\ \hline & & & & 0 & c & a_{+3} & c & 0 & \\ & & & & & \ddots & \ddots & \ddots & \ddots & \ddots \end{pmatrix} \begin{pmatrix} \vdots \\ b_{-3} \\ \hline b_{-1} \\ b_{+1} \\ \hline b_{+3} \\ \vdots \end{pmatrix} = -\frac{\mathrm{i}\Omega}{2} \begin{pmatrix} \vdots \\ 0 \\ \hline 1 \\ 1 \\ \hline 0 \\ \vdots \end{pmatrix}, \tag{A5}$$

with $a_n = [\gamma + \mathrm{i}(\Delta_a + k_c n v)] + g^2/(2\kappa)$ and $c = g^2/(4\kappa)$. Neglecting couplings to harmonics of higher order ($b_{|n|>1} = 0$) reduces the problem to a 2×2 linear system with coupled coefficients $b_{\pm 1}$,

$$\begin{pmatrix} a_{-1} & c \\ c & a_{+1} \end{pmatrix} \begin{pmatrix} b_{-1} \\ b_{+1} \end{pmatrix} = -\frac{\mathrm{i}\Omega}{2} \begin{pmatrix} 1 \\ 1 \end{pmatrix}. \tag{A6}$$

Inverting this matrix yields the solution

$$b_{\pm 1} = -\frac{\mathrm{i}\Omega}{2[\gamma(1+\mathcal{C}/4) + \mathrm{i}(\Delta_a \pm k_c v)]} \left[1 + \sum_{\pm} \frac{g^2}{4\kappa} \frac{1}{[\gamma(1+\mathcal{C}/4) + \mathrm{i}(\Delta_a \pm k_c v)]}\right]^{-1}. \tag{A7}$$

Expansion to first order in $k_c v/\Delta_a$ gives

$$b_{\pm 1} \approx -\frac{\mathrm{i}\Omega}{2[\gamma(1+3\mathcal{C}/4) + \mathrm{i}\Delta_a]} \pm \frac{-\Omega}{2[\gamma(1+\mathcal{C}/4) + \mathrm{i}\Delta_a][\gamma(1+3\mathcal{C}/4) + \mathrm{i}\Delta_a]} k_c v. \tag{A8}$$

However, one is not restricted to the approximation of two sidebands only, which holds for free space emitters but not when taking into account the interaction with the cavity for $\mathcal{C}\gamma/\Delta \gg 1$. We can cast the equations for the steady-state Floquet coefficients in the following form

$$(\boldsymbol{A} + \mathrm{i}k_c v \boldsymbol{D})\vec{b} = \vec{\Omega}, \tag{A9}$$

with $\boldsymbol{A}$ a symmetric tridiagonal Toeplitz matrix, $\boldsymbol{D}$ a diagonal matrix and $\vec{\Omega} = -\mathrm{i}\Omega(\delta_{n,+1} + \delta_{n,-1})/2$ the drive of the spatial harmonics of first order. In matrix notation

$$\left[\begin{pmatrix} \ddots & \ddots & \ddots & \ddots & \ddots & & & & \\ & 0 & c & a & c & 0 & & & \\ & & 0 & c & a & c & 0 & & \\ & & & 0 & c & a & c & 0 & \\ & & & & 0 & c & a & c & 0 \\ & & & & & \ddots & \ddots & \ddots & \ddots & \ddots \end{pmatrix} + \mathrm{i}k_c v \begin{pmatrix} \ddots & & & & & \\ & -3 & & & & \\ & & -1 & & & \\ & & & +1 & & \\ & & & & +3 & \\ & & & & & \ddots \end{pmatrix}\right] \begin{pmatrix} \vdots \\ b_{-3} \\ b_{-1} \\ b_{+1} \\ b_{+3} \\ \vdots \end{pmatrix} = -\frac{\mathrm{i}\Omega}{2} \begin{pmatrix} \vdots \\ 0 \\ 1 \\ 1 \\ 0 \\ \vdots \end{pmatrix}, \tag{A10}$$

with $a = (\gamma + \mathrm{i}\Delta_a) + g^2/(2\kappa)$ and $c = g^2/(4\kappa)$. As we are merely interested in a solution to linear order in $k_c v/\Delta_a$, which gives the cooling or friction-like force, we take a perturbative approach in the Doppler shift

$$\vec{b} = [\boldsymbol{A} + \mathrm{i}k_c v \boldsymbol{D}]^{-1}\vec{\Omega} \approx [\boldsymbol{A}^{-1} - \mathrm{i}k_c v \boldsymbol{A}^{-1}\boldsymbol{D}\boldsymbol{A}^{-1}]\vec{\Omega} = \vec{b}^{(0)} - \mathrm{i}k_c v \vec{b}^{(1)}. \tag{A11}$$

The emitter coherence can then be written as

$$\beta = \sum_{n=-\infty}^{\infty} b_{2n+1} \mathrm{e}^{\mathrm{i}k_c(2n+1)x} = \sum_{n=0}^{\infty} \left\{2b_{2n+1}^{(0)} \cos[(2n+1)k_c x] + 2k_c v b_{2n+1}^{(1)} \sin[(2n+1)k_c x]\right\}. \tag{A12}$$

For sufficiently high harmonic order n the perturbative expansion in the Doppler shift breaks down since the perturbation diverges, i.e., $nk_c v/\Delta_a > 1$ for some n. However, from the formal integration of α to order g/κ we obtain the force

$$\begin{aligned}\dot{p} &= -\hbar g'(x)[\beta\alpha^* + \beta^*\alpha] \\ &= \hbar g k_c \sin(k_c x)\bigg[\beta\bigg(-\frac{\eta}{\kappa - \mathrm{i}\Delta_c} + \frac{\mathrm{i}g(x)}{\kappa - \mathrm{i}\delta}\beta^*\bigg) \\ &\quad + \beta^*\bigg(-\frac{\eta}{\kappa + \mathrm{i}\Delta_c} - \frac{\mathrm{i}g(x)}{\kappa + \mathrm{i}\delta}\beta\bigg)\bigg], \end{aligned} \tag{A13}$$

such that for $\delta = 0$ we obtain the spatially averaged force $\dot{p} \approx 2\hbar k_c^2 v \Im(\Omega^* b_{+1}^{(1)})$. So when the cavity is resonant with the emitter only coefficients $b_n^{(1)}$ with $n = \pm 1$ contribute with nonzero spatial average. This justifies the perturbative approach. The elements of the inverse of the tridiagonal Toeplitz operator $\boldsymbol{A}$ are given by [31]

$$\langle i|\boldsymbol{A}^{-1}|j\rangle = \frac{4\kappa}{g^2}\frac{\lambda^{|i-j|+1}}{\lambda^2 - 1}, \tag{A14}$$

with

$$\begin{aligned}\lambda &= (-a + \sqrt{a^2 - 4c^2})/(2c) \\ &= -1 - \frac{2\kappa(\gamma + \mathrm{i}\Delta_a)}{g^2}\left(1 - \sqrt{1 + \frac{g^2}{\kappa(\gamma + \mathrm{i}\Delta_a)}}\right). \end{aligned} \tag{A15}$$

The coefficients are given by

$$b_{2n+1}^{(0)} = -\frac{\mathrm{i}\Omega}{2}\frac{4\kappa}{g^2}\frac{\lambda^{n+1}}{\lambda - 1} \quad \text{with } n \in \mathbb{N}, \tag{A16a}$$

$$b_{+1}^{(1)} = -\frac{\mathrm{i}\Omega}{2}\left(\frac{4\kappa}{g^2}\right)^2\frac{\lambda^2(\lambda^2 + 1)}{(\lambda^2 - 1)^3}. \tag{A16b}$$

The Floquet coefficients $b_{2n+1}^{(0)}$ will be relevant for the population transfer in the nonclosed transition system and the coefficient $b_{+1}^{(1)}$ gives the cooling rate.

2. Single nonclosed transition system inside a cavity

The Floquet coefficients of first order to leading order in $k_c v/\Delta_a$ now have the following grounds-state dependency:

$$\begin{aligned} b_{\pm 1} \approx &-\frac{\mathrm{i}\Omega n_g}{2[\gamma(1 + 3\mathcal{C}n_g/4) + \mathrm{i}\Delta_a]} \\ &\pm \frac{-\Omega n_g}{2[\gamma(1 + \mathcal{C}n_g/4) + \mathrm{i}\Delta_a][\gamma(1 + 3\mathcal{C}n_g/4) + \mathrm{i}\Delta_a]}k_c v. \end{aligned} \tag{A17}$$

The differential equation for the ground state under steady-state assumption for the excited state $\dot{n}_e = 0$ is given by

$$\dot{n}_g = -\frac{|\Omega|^2\gamma' n_g}{\gamma_{\text{tot}}^2(1 + n_g 3\mathcal{C}/4)^2 + \Delta_a^2}. \tag{A18}$$

This equation is separable and integrable, but not solvable for $n_g(t)$. We thus determine the final velocity when all population is lost to the intermediate state

$$v(t \to \infty) = v_0 \exp\left[-\int_0^\infty \xi(n_g(t))dt\right]. \tag{A19a}$$

We solve the integral by carrying out the integration over the ground-state population with $n_g(0) = 1$ and $n_g(t \to \infty) = 0$,

$$\begin{aligned}\int_0^\infty \xi_c(n_g(t))dt &= \int_1^0 \xi_c(n_g)\frac{dt}{dn_g}dn_g \\ &= \frac{2\hbar k_c^2\Delta_a\gamma_{\text{tot}}}{\gamma'\Delta_a^2}\int_0^1 \frac{(1 + \mathcal{C}/2n_g)}{\left[1 + \frac{\gamma_{\text{tot}}^2}{\Delta_a^2}(1 + \mathcal{C}n_g/4)^2\right]}dn_g \\ &\approx \frac{4\omega_{\text{rec.}}\Delta_a\gamma_{\text{tot}}}{\gamma'(\gamma_{\text{tot}}^2 + \Delta_a^2)}\left[1 + \frac{\mathcal{C}\Delta_a^2}{4(\Delta_a^2 + \gamma_{\text{tot}}^2)}\right], \end{aligned} \tag{A20}$$

where the last step is a Taylor expansion in $\mathcal{C}\gamma_{\text{tot}}/\Delta_a \ll 1$, which is already required for the cut-off of the Floquet expansion.

We can consider the population dynamics without restriction to the two-dimensional system of Floquet coefficients, i.e., consider the Floquet coefficients given by Eq. (A16). Elimination of the excited state $\dot{n}_e = 0$ yields

$$\dot{n}_g = -\frac{\gamma'}{\gamma_{\text{tot}}}\mathrm{i}g(x)[\beta\alpha^* - \beta^*\alpha], \tag{A21a}$$

$$\dot{n}_i = \frac{\gamma'}{\gamma_{\text{tot}}}\mathrm{i}g(x)[\beta\alpha^* - \beta^*\alpha], \tag{A21b}$$

where we insert the formal integration for the cavity mode to obtain

$$\dot{n}_g = \frac{\gamma'}{\gamma_{\text{tot}}}\left[2\Im(\Omega^*(x)\beta) + \frac{2g^2(x)}{\kappa}|\beta|^2\right]. \tag{A22}$$

As β now contains all Floquet coefficients $2n + 1$ with $n \in \mathbb{N}$, calculating the second term in the drive $\propto g^2(x)|\beta|^2$ leads to geometric series. Once again invoking the previous argument that we can perform a spatial average to keep only constant terms

$$\begin{aligned}\langle g^2(x)|\beta|^2\rangle_x = \frac{g^2}{2}\sum_{m=0}^\infty \big[&b_{2m+1}^{(0)}b_{2m+1}^{(0)*}\delta_{m,0} + 2b_{2m+1}^{(0)}b_{2m+1}^{(0)*} \\ &+ b_{2m+3}^{(0)}b_{2m+1}^{(0)*} + b_{2m+1}^{(0)}b_{2m+3}^{(0)*}\big]. \end{aligned} \tag{A23}$$

Calculating the geometric series we obtain the differential equation for the ground state

$$\dot{n}_g = \frac{\gamma'}{\gamma_{\text{tot}}}\frac{2\kappa|\Omega|^2}{g^2}\frac{|\lambda^2|(4 + \lambda + \lambda^*) + \lambda + \lambda^*}{|\lambda - 1|^2(1 - |\lambda|^2)}, \tag{A24}$$

where λ now has the following ground-state dependency:

$$\lambda = -1 - \frac{2\kappa(\gamma_{\text{tot}} + \mathrm{i}\Delta_a)}{g^2 n_g}\left(1 - \sqrt{1 + \frac{g^2 n_g}{\kappa(\gamma_{\text{tot}} + \mathrm{i}\Delta_a)}}\right). \tag{A25}$$

APPENDIX B: DOPPLER COOLING OF $\mathcal{N}$ QUANTUM EMITTERS

We now proceed with the treatment of an arbitrary number of emitters $\mathcal{N}$. As stated in the main text, we then assume that the single-particle cooperativity is small $\mathcal{C} \ll 1$, whereas the collective cooperativity $\mathcal{C}\mathcal{N} \gg 1$ is large.

1. $\mathcal{N}$ closed transition emitter inside a cavity

Formally integrating and inserting α into the equation of motion for β_j and expanding it in the Floquet coefficients of the cavity field

$$\beta_j = \sum_{n=-\infty}^{\infty} b_{j,n} \mathrm{e}^{\mathrm{i}nk_c x_j}, \tag{B1}$$

leads to the following set of coupled equations for the steady-state Floquet coefficient $b_{j,n}$ for particle j of the nth-order harmonic

$$\begin{aligned}
&b_{j,n}[\gamma + \mathrm{i}(\Delta_a + nk_c v_j)] \\
&= -\frac{\mathrm{i}\Omega}{2}(\delta_{n,+1} + \delta_{n,-1}) - \frac{g^2}{4\kappa}\sum_{i=1}^{\mathcal{N}}\sum_{m=-\infty}^{\infty} b_{i,m}\big[\mathrm{e}^{\mathrm{i}k_c[(m+1)x_i-(n-1)x_j]} + \mathrm{e}^{\mathrm{i}k_c[(m+1)x_i-(n+1)x_j]} + \mathrm{e}^{\mathrm{i}k_c[(m-1)x_i-(n-1)x_j]} + \mathrm{e}^{\mathrm{i}k_c[(m-1)x_i-(n+1)x_j]}\big] \\
&\approx -\frac{\mathrm{i}\Omega}{2}(\delta_{n,+1} + \delta_{n,-1}) \\
&\quad - \frac{g^2}{4\kappa}\sum_{i=1}^{\mathcal{N}}\sum_{m=-\infty}^{\infty} b_{i,m}\big[\mathrm{e}^{\mathrm{i}k_c[(m+1)v_i-(n-1)v_j]t} + \mathrm{e}^{\mathrm{i}k_c[(m+1)v_i-(n+1)v_j]t} + \mathrm{e}^{\mathrm{i}k_c[(m-1)v_i-(n-1)v_j]t} + \mathrm{e}^{\mathrm{i}k_c[(m-1)v_i-(n+1)v_j]t}\big] \\
&\approx -\frac{\mathrm{i}\Omega}{2}(\delta_{n,+1} + \delta_{n,-1}) \; - \frac{g^2}{4\kappa}[b_{j,n-2} + b_{j,n+2} + 2b_{j,n}] - \frac{g^2}{4\kappa}\sum_{i\neq j}^{\mathcal{N}}[\delta_{n,1}(b_{i,1} + b_{i,-1}) + \delta_{n,-1}(b_{i,1} + b_{i,-1})].
\end{aligned} \tag{B2}$$

From numerical simulations we find that this holds in the relevant parameter regime, i.e., for small single-particle cooperativity $\mathcal{C} \ll 1$, such that Floquet coefficients $b_{j,n}$ with $|n| > 1$ can be neglected. Under the restriction to Floquet coefficients of first order $b_{j,\pm 1}$ these equations may be cast into matrix form, as shown in Eq. (28), and inverted using the Sherman-Morrison formula. From this procedure we obtain the expression

$$b_{j,\pm 1} = -\frac{\mathrm{i}\Omega}{2}\frac{1}{\gamma(1+\mathcal{C}/4) + \mathrm{i}(\Delta_a \pm k_c v_j)}\left[1 + \frac{g^2}{4\kappa}\sum_{m,\pm}^{\mathcal{N}}\frac{1}{[\gamma(1+\mathcal{C}/4) + \mathrm{i}(\Delta_a \pm k_c v_m)]}\right]^{-1}. \tag{B3}$$

Expanding the coefficient $b_{j,\pm 1}$ for particle j up to first order in all velocities $k_c v_i/\Delta_a$ gives

$$b_{j,\pm 1} \approx -\frac{\mathrm{i}\Omega}{2}\frac{1}{\gamma(1+\mathcal{C}(2\mathcal{N}+1)/4) + \mathrm{i}\Delta_a} \pm \frac{-\Omega}{2}\frac{1}{[\gamma(1+\mathcal{C}/4) + \mathrm{i}\Delta_a][\gamma(1+\mathcal{C}(2\mathcal{N}+1)/4) + \mathrm{i}\Delta_a]}k_c v_j, \tag{B4}$$

which shows a collectively modified decay rate, similar to the single-particle case [see Eq. (A8)]. Inserting this solution into the steady-state solution for α gives

$$\alpha \approx -\frac{\eta}{\kappa + \mathrm{i}\Delta_c} - \frac{\mathrm{i}g\mathcal{N}b^{(0)}}{\kappa} = -\frac{\eta}{\kappa + \mathrm{i}\Delta_c}\left[1 - \frac{g^2\mathcal{N}}{2\kappa}\frac{1}{\gamma(1+(2\mathcal{N}+1)\mathcal{C}/4) + \mathrm{i}\Delta_a}\right], \tag{B5}$$

where we invoke the spatial averaging argument again, for $\mathcal{N}$ spatial variables x_j this time. The amplitude of the cavity field is now reduced.

2. $\mathcal{N}$ nonclosed transition systems inside a cavity

The final velocity reached inside the cavity can be calculated analogous to the single-particle case. The collective modifications cancel in the final velocity leaving only single-particle effects. Explicitly we obtain

$$\begin{aligned}
\int_0^\infty \xi_c(n_g(t))dt &= \int_1^0 \xi_c(n_g)\frac{dt}{dn_g}dn_g \\
&= \frac{8\hbar k_c^2\gamma_{\mathrm{tot}}}{m\gamma'}\int_0^1 \frac{(1+n_g\mathcal{C}/2)\big[\Delta_a^2 + \gamma_{\mathrm{tot}}^2(1+n_g(2\mathcal{N}+1)\mathcal{C}/4)^2\big]}{\big[\Delta_a^2 + \gamma_{\mathrm{tot}}^2(1+n_g\mathcal{C}/4)^2\big]\big[\Delta_a^2 + \gamma_{\mathrm{tot}}^2(1+n_g(2\mathcal{N}+1)\mathcal{C}/4)^2\big]}dn_g \\
&= \frac{4\omega_{\mathrm{rec.}}\Delta_a\gamma_{\mathrm{tot}}}{\gamma'\Delta_a^2}\int_0^1 \frac{(1+n_g\mathcal{C}/2)}{\Big[1 + \frac{\gamma_{\mathrm{tot}}^2}{\Delta_a^2}(1+n_g\mathcal{C}/4)^2\Big]}dn_g,
\end{aligned} \tag{B6}$$

which is now equivalent to the single emitter case.

[1] D. J. Wineland and W. M. Itano, Laser cooling, Phys. Today **40**(6), 34 (1987).
[2] S. Chu and C. Wieman, Laser cooling and trapping of atoms: Introduction, J. Opt. Soc. Am. B **6**, 2020 (1989).
[3] C. N. Cohen-Tannoudji and W. D. Phillips, New mechanisms for laser cooling, Phys. Today **43**(10), 33 (1990).
[4] C. E. Wieman, D. E. Pritchard, and D. J. Wineland, Atom cooling, trapping, and quantum manipulation, Rev. Mod. Phys. **71**, S253 (1999).
[5] P. Berman, *Cavity Quantum Electrodynamics*, Advances in Atomic, Molecular, and Optical Physics (Academic Press, New York, 1994).
[6] S. Haroche and D. Kleppner, Cavity quantum electrodynamics, Phys. Today **42**(1), 24 (1989).
[7] H. Walther, B. T. Varcoe, B. Englert, and T. Becker, Cavity Quantum Electrodynamics, Rep. Prog. Phys. **69**, 1325 (2006).
[8] S. Haroche and J.-M. Raimond, *Exploring the Quantum: Atoms, Cavities, and Photons* (Oxford University Press, New York, 2013).
[9] P. Horak, G. Hechenblaikner, K. M. Gheri, H. Stecher, and H. Ritsch, Cavity-induced atom cooling in the strong coupling regime, Phys. Rev. Lett. **79**, 4974 (1997).
[10] V. Vuletić and S. Chu, Laser cooling of atoms, ions, or molecules by coherent scattering, Phys. Rev. Lett. **84**, 3787 (2000).
[11] P. Domokos and H. Ritsch, Mechanical effects of light in optical resonators, J. Opt. Soc. Am. B **20**, 1098 (2003).
[12] H. Ritsch, P. Domokos, F. Brennecke, and T. Esslinger, Cold atoms in cavity-generated dynamical optical potentials, Rev. Mod. Phys. **85**, 553 (2013).
[13] P. Maunz, T. Puppe, I. Schuster, N. Syassen, P. W. H. Pinkse, and G. Rempe, Cavity cooling of a single atom, Nature (London) **428**, 50 (2004).
[14] M. Wolke, J. Klinner, H. Keßler, and A. Hemmerich, Cavity cooling below the recoil limit, Science **337**, 75 (2012).
[15] H. W. Chan, A. T. Black, and V. Vuletić, Observation of collective-emission-induced cooling of atoms in an optical cavity, Phys. Rev. Lett. **90**, 063003 (2003).
[16] M. Hosseini, Y. Duan, K. M. Beck, Y.-T. Chen, and V. Vuletić, Cavity cooling of many atoms, Phys. Rev. Lett. **118**, 183601 (2017).
[17] B. L. Lev, A. Vukics, E. R. Hudson, B. C. Sawyer, P. Domokos, H. Ritsch, and J. Ye, Prospects for the cavity-assisted laser cooling of molecules, Phys. Rev. A **77**, 023402 (2008).
[18] E. S. Shuman, J. F. Barry, and D. DeMille, Laser cooling of a diatomic molecule, Nature (London) **467**, 820 (2010).
[19] V. Zhelyazkova, A. Cournol, T. E. Wall, A. Matsushima, J. J. Hudson, E. A. Hinds, M. R. Tarbutt, and B. E. Sauer, Laser cooling and slowing of CaF molecules, Phys. Rev. A **89**, 053416 (2014).
[20] S. Truppe, H. J. Williams, M. Hambach, L. Caldwell, N. J. Fitch, E. A. Hinds, B. E. Sauer, and M. R. Tarbutt, Molecules cooled below the doppler limit, Nat. Phys. **13**, 1173 (2017).
[21] L. Anderegg, B. L. Augenbraun, Y. Bao, S. Burchesky, L. W. Cheuk, W. Ketterle, and J. M. Doyle, Laser cooling of optically trapped molecules, Nat. Phys. **14**, 890 (2018).
[22] D. Mitra, N. B. Vilas, C. Hallas, L. Anderegg, B. L. Augenbraun, L. Baum, C. Miller, S. Raval, and J. M. Doyle, Direct laser cooling of a symmetric top molecule, Science **369**, 1366 (2020).
[23] B. L. Augenbraun, J. M. Doyle, T. Zelevinsky, and I. Kozyryev, Molecular asymmetry and optical cycling: Laser cooling asymmetric top molecules, Phys. Rev. X **10**, 031022 (2020).
[24] D. Wang, H. Kelkar, D. Martin-Cano, D. Rattenbacher, A. Shkarin, T. Utikal, S. Götzinger, and V. Sandoghdar, Turning a molecule into a coherent two-level quantum system, Nat. Phys. **15**, 483 (2019).
[25] D. Walls and G. Milburn, *Quantum Optics* (Springer, Berlin, 2008).
[26] M. O. Scully and M. S. Zubairy, *Quantum Optics* (American Association of Physics Teachers, College Park, MD, 1999).
[27] P. Meystre and M. Sargent, *Elements of Quantum Optics* (Springer Science & Business Media, New York, 2007).
[28] G. Grynberg, A. Aspect, and C. Fabre, *Introduction to Quantum Optics: From the Semi-Classical Approach to Quantized Light* (Cambridge University Press, Cambridge, England, 2010).
[29] C. Gardiner and P. Zoller, *The Quantum World of Ultra-Cold Atoms and Light Book II: The Physics of Quantum-Optical Devices* (World Scientific, Singapore, 2015), Vol. 4.
[30] S. Jack and M. Winifred J., Adjustment of an inverse matrix corresponding to changes in the elements of a given column or a given row of the original matrix, Ann. Math. Stat. **20**, 621 (1949).
[31] F. R. Klausen and A. H. Werner, Spectra of generators of Markovian evolution in the thermodynamic limit: From non-Hermitian to full evolution via tridiagonal Laurent matrices, arXiv:2206.09879.